Biofilm 9 (2025) 100258

Contents lists available at ScienceDirect

Biofilm

journal homepage: www.sciencedirect.com/journal/biofilm

Legionella pneumophila response to shifts in biofilm structure mediated by hydrodynamics

Ana Rosa Silva [a,b], C. William Keevil [c], Ana Pereira [a,b,*]

[a] LEPABE - Laboratory for Process Engineering, Environment, Biotechnology and Energy, Faculty of Engineering, University of Porto, Rua Dr. Roberto Frias, 4200-465, Porto, Portugal
[b] ALiCE - Associate Laboratory in Chemical Engineering, Faculty of Engineering, University of Porto, Rua Dr. Roberto Frias, 4200-465, Porto, Portugal
[c] School of Biological Sciences, University of Southampton, Southampton, United Kingdom

ARTICLE INFO

Keywords:
Biofilm structural changes
Flow regime
Legionella pneumophila migration
Stagnation
VBNC

ABSTRACT

Preventing legionellosis in water systems demands effective hydrodynamic management and biofilm mitigation. This study investigates the complex relationship between hydrodynamics (80 RPM and stagnation), biofilm mesoscale structure and *Legionella pneumophila* colonization, by addressing three key questions: (1) How do low flow *vs* stagnation conditions affect biofilm response to *L. pneumophila* colonization?, (2) How do biofilm structural variations mediate *L. pneumophila* migration across the biofilm?, and (3) Can specific hydrodynamic conditions trigger *L. pneumophila* entrance in a viable but nonculturable (VBNC) state? It was found that *Pseudomonas fluorescens* biofilms exhibit different responses to *L. pneumophila* based on the prevailing hydrodynamic conditions. While biofilm thickness and porosity decreased under shear (80 RPM), thickness tends to significantly increase when pre-established 80 RPM-grown biofilms are set to stagnation upon *L. pneumophila* spiking. Imposing stagnation after the spiking also seemed to accelerate *Legionella* migration towards the bottom of the biofilm. Water structures in the biofilm seem to be key to *Legionella* migration across the biofilm. Finally, shear conditions favoured the transition of *L. pneumophila* to VBNC states (~94 %), despite the high viable cell counts (~8 $\log_{10}$ CFU/cm^2) found throughout the experiments. This research highlights the increased risk posed by biofilms and stagnation, emphasizing the importance of understanding the mechanisms that govern *Legionella* behaviour in diverse biofilm environments. These insights are crucial for developing more effective monitoring and prevention strategies in water systems.

1. Introduction

The widespread occurrence of *Legionella* in water systems poses significant public health risks [1]. Legionellosis cases are increasing worldwide and are likely to keep rising due to societal challenges [2]. Climate changes [3], urbanization leading to more complex water systems [4,5], and increased water reuse [6] are expected to be key contributors to *Legionella* proliferation in field-engineered systems. Simultaneously, a growing population of immunosuppressed individuals and the ageing demographic increase susceptibility to infection [7].

These challenges underscore the need for strengthened *Legionella* management practices in water systems [1]. Beyond *Legionella* physiological adaptations, including its ability to enter a viable but nonculturable (VBNC) state [8], *Legionella*'s settlement is influenced by external factors such as temperature [9], nutrients [10], hydrodynamic conditions [11–13], and the presence of protozoa and biofilms within the microbial ecosystem [12,14–17].

Multiple factors interact to shape *Legionella* behaviour within water systems. For instance, hydrodynamics significantly influences biofilm structure, affecting attributes like thickness, density, and porosity [18,19], as well as the microbiome composition of the biofilm [20]. Fluid shear forces facilitate the mass transfer of nutrients and oxygen, leading to thinner and less porous biofilms under higher shear stresses compared to those formed under lower forces [21–23]. Moreover, stagnation is associated with increased risks of *Legionella* prevalence in water systems [24], adversely impacting water quality [25] and promoting biofilm development alongside *Legionella* settlement [13,14].

An increasing number of studies have been exploring the interactions

* Corresponding author. LEPABE - Laboratory for Process Engineering, Environment, Biotechnology and Energy, Faculty of Engineering, University of Porto, Rua Dr. Roberto Frias, 4200-465, Porto, Portugal.
E-mail address: aalex@fe.up.pt (A. Pereira).

https://doi.org/10.1016/j.bioflm.2025.100258
Received 6 December 2024; Received in revised form 16 January 2025; Accepted 24 January 2025
Available online 24 January 2025

between *Legionella* and biofilms [2,14,26,27] regarding environmental changes. Recent findings by Margot et al. (2024) reveal that multispecies biofilm development in new plumbing materials changes over time, with *Legionella* emerging as an early colonizer [2]. Similarly, Cavallaro et al. (2023) noted that the microbiome constituents of biofilms can influence *Legionella* abundance in shower hoses [26].

Despite these advancements, many studies still rely on microbial analyses accomplished by disrupting the biofilm matrix [2,28]. Such approaches ignore the importance of the three-dimensional (3D) biofilm structure, a crucial characteristic of biofilms. The biofilm 3D matrix confers protection to microorganisms [29], enables microbial interactions such as co-aggregation and gene transfer, and cell-to-cell communication, and its viscoelastic properties provide flexibility to adapt to environmental changes [30–32]. Shen et al. (2015) highlighted that biofilm roughness is crucial for *Legionella* adhesion [11], while Silva et al. (2024) demonstrated that *L. pneumophila* migrates through the structure of *P. fluorescens* biofilms to the bottom in just a few hours, remaining cultivable for several days [14].

Furthermore, the mesoscale structure of biofilms is vital for understanding their mechanics and interactions with the environment [33]. However, the behaviour of biofilms in the presence of *L. pneumophila*, and the bacterium's response to different biofilm structures influenced by hydrodynamic conditions, remains poorly understood.

This study investigates how the mesoscale structure of biofilms, influenced by different hydrodynamic conditions (80 RPM and stagnation), impacts *L. pneumophila* in three key ways: (i) how the biofilm rearranges upon *L. pneumophila* entry, (ii) how it affects *Legionella* migration within the biofilm, and (iii) how it triggers the bacterium's transition into a VBNC state.

2. Materials and methods

The 12-well plate platform designed for controlled experiments was used [14]. *P. fluorescens* biofilms were grown in this laboratory setup under dynamic conditions – 80 RPM. On the third day, *L. pneumophila* was spiked into the system, and colonization started. Following the spiking, two hydrodynamic conditions were examined: maintaining shear at 80 RPM and shifting from 80 RPM to stagnation. Optical Coherence Tomography (OCT) was used to analyse the biofilm's mesoscale structure, while *L. pneumophila* was labelled with a specific 16S rRNA peptide nucleic acid (PNA) probe to track its spatial position using Confocal Laser Scanning Microscopy (CLSM). By combining the Direct Viable Count (DVC) technique with PNA hybridization, it was possible to quantify the number of VBNC cells over time.

2.1. Bacterial strains and cultivation

P. fluorescens ATCC 13525^{T} (*Pf*) was used as a biofilm-forming organism and *L. pneumophila* serogroup 1 (WDCM00107) (*Lp*) was used to spike the pre-established *Pf* biofilms. The *Pf* bacterium was cultivated overnight at 30 ± 3 °C under agitation in sterile R2 medium, which consists of, per liter, 0.5 g peptone, 0.5 g glucose, 0.1 g magnesium sulphate · $7H_2O$, 0.3 g sodium pyruvate, 0.5 g yeast extract, 0.5 g casein hydrolysate, 0.5 g starch soluble and 0.393 g di-potassium · $3H_2O$ (Merck, Portugal). *L. pneumophila* was cultivated on buffered charcoal-yeast extract (BCYE) agar (Merck, Portugal) at 37 °C for 2 days.

2.2. Biofilm formation

Biofilms were developed on 12-well microtiter plates (VWR International, Portugal), since this platform was shown to be suitable for *Legionella*-biofilm interaction studies [14].

P. fluorescens was chosen as the biofilm-forming species due to its ubiquity in biofilms of engineered water systems [34] and it is very well characterized [14,19,35]. The *Pf* biofilm was grown in 12-well plates, using polyvinyl chloride (PVC) coupons as reported by Silva et al. (2024) [14]. Briefly, it consisted of harvesting the overnight *Pf* culture by centrifuging it, followed by adjusting their OD_{600} to reach 10^8 CFU/mL in fresh R2. Afterwards, 3 mL of the *Pf* bacterial suspension were placed in each well and the plates were incubated at 30 °C in an orbital shaker with a 25 mm orbital diameter (New Brunswick Innova 44, Eppendorf, Portugal) at 80 RPM (corresponding to a shear rate in the range of 4 and 40 s^{-1} [36]). Three days later, a suspension of *Lp* (10^9 CFU/mL in distilled water) was spiked to the pre-established biofilms. The plates were reincubated either under the same flow regime (80 RPM) or stagnation (80 RPM – Stag). The bulk media was renewed every 2 days. The experimental design depicted in Fig. 1 was implemented.

2.3. Biofilm analysis

The biofilms were analyzed prior to and after *L. pneumophila* spiking. Briefly, the bulk medium was removed from the wells and the biofilms were gently washed with sterile saline solution (8.5 g/L NaCl) to eliminate the loosely attached cells. The coupons to be imaged with OCT were kept in the wells with 3 mL of saline solution, and those to be imaged with confocal laser scanning microscopy (CLSM) were set to air dry. For the quantification of sessile cells, the coupons were removed from the wells and placed in 15-mL Falcon tubes with 2 mL of saline solution where biofilm disaggregation was made through three alternate cycles of 30 s sonicating (Ultrasonic Cleaner USC-T, 45 kHz, VWR International, Portugal) and vortexing.

2.3.1. Optical coherence tomography (OCT)

Biofilms were imaged using spectral-domain Optical Coherence Tomography (OCT; Thorlabs GmbH, Germany) as previously described [14]. The captured volume was 2.49 × 2.13 × 1.52 mm. For each coupon under analysis, the 2D imaging was performed with a minimum of six fields of view, while for the 3D imaging (corresponding to 509 stacks), a minimum of three fields of view were acquired. The images were then processed with Biofilm Imaging and Structure Classification Automatic Processor (BISCAP software) [37,38], where pixel intensity thresholds were applied to binarize pixels as biomass or background, distinguishing the biofilm from the liquid phase. The biofilm thickness (distance between the biofilm's top and bottom) and porosity (fraction of empty spaces within the biofilms) were quantified with BISCAP. Representative 3D – OCT images (composed by the 509 stacks) were selected for the desired conditions and videos were set with 200 out of the 509 stacks using the Fiji software.

2.3.2. Confocal laser scanning microscopy (CLSM)

The migration of *Lp* (both under 80 RPM – 80 RPM and 80 RPM – Stag) within the pre-established *Pf* biofilms was tracked over 24 h by removing biofilm coupons from the plates at the following timepoints: 5, 15, 30 and 45 min, and then every hour after spiking until the 24 h. *Lp* was successfully stained red using a 16S rRNA PNA probe as already reported [14,39]. Biofilm samples were observed using a helium-neon laser at 565 nm and a 405-diode at 398 nm and using a 60 × water objective lens (Leica HC PL APO CS, Leica Microsystems, Germany) in an inverted microscope Leica DMI6000-CS. A minimum of three z-stacks of horizontal plane images (512 × 512 pixels, corresponding to 387.5 × 387.5 μm) with a z-step of 0.36 μm were captured. For image analysis, green corresponds to *P. fluorescens* cells (due to the auto-fluorescence conferred by the production of pyoverdines [40]) and red corresponds

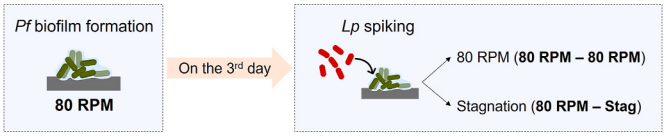

Fig. 1. Schematic representation of experimental design adopted in the present study.

to *L. pneumophila*.

Three-dimensional (3D) projections of biofilm structures were reconstructed from z-stacks using the "Easy 3D" tool in IMARIS 9.1 software (Bitplane, Switzerland). The orthogonal perspectives were also obtained. To quantify the biovolume (the total volume of biomass, μm^3, in a given area of the biofilm, divided by the substratum surface area, μm^2) of each bacterium, the COMSTAT2 plugin for ImageJ was used.

2.3.3. Quantification of sessile and planktonic cells

The culturability of *P. fluorescens* was assessed by plating the appropriate serial dilutions in plate count agar (PCA) (Oxoid, Portugal), following incubation at 30 °C for 24 h. Afterwards, the biofilm suspensions were subjected to 50 °C for 30 min (to eliminate *P. fluorescens* from the sample), spread onto BCYE-GVPC (buffered charcoal yeast extract supplemented with glycine, vancomycin, polymyxin and cycloheximide) selective agar medium and incubated at 37 °C up to 10 days to assess *Legionella* culturability.

To quantify the total number of *L. pneumophila* cells, the PNA probe PLPNE620 was used in a FISH assay. Briefly, 25 μL of an appropriate dilution was deposited on the wells of hybridization slides and let to air dry. The slides were then flamed three times, covered with 90 % (v/v) ethanol and air dried, allowing cell fixation. The hybridization and washing was performed as described previously [41]. After the FISH assay, the slides were dried and a drop of nonfluorescent immersion oil (Sigma, Portugal) was put onto the slide and a coverslip was placed on the top. Then, another drop of immersion oil was placed on the objective and slides were observed using a Nikon Eclipse Ti SR inverted epifluorescence microscope (Nikon Instruments, Netherlands) using 40 × Plan APO objectives (Nikon Instruments). The microscope was connected to a DS-Ri2 camera (Nikon Instruments).

2.3.4. Viable but nonculturable L. pneumophila

Direct viable count (DVC) was used to enumerate *Lp* VBNC cells. The DVC-FISH method allowed a fast and specific detection of viable *L. pneumophila* cells, overcoming the limitations of other methods, such as the need for DNA extraction and lack of specificity for *Legionella*. One mL of the biofilm or bulk sample was added to 4 mL of sterile distilled water and to 5 mL of R2 media. Pipemidic acid – the antibiotic that inhibits cell division, thus allowing the viable cells to elongate [42] – was added at a final concentration of 10 μg/mL. Samples were then incubated overnight at 37 °C under agitation. Afterwards, samples were hybridized and observed under the microscope as aforementioned. The cells that have elongated, at least twice their original size, were considered viable. The percentage of VBNC cells was calculated as the difference between the numbers of viable and culturable cells in relation to total *Lp* cell counts, as the equation below.

$$\%\text{VBNC} = \frac{\text{Viable cells} - \text{CFU}}{\text{Total cells}} \times 100$$

2.4. Statistical analysis

The obtained data were further analyzed by the software GraphPad Prism 9.0 for Windows (GraphPad Software, USA). To ensure the accuracy of the data obtained, three independent experiments were performed with two biological replicates. The mean and standard deviation (SD) for each considered parameter were calculated. An ANOVA single-factor statistical analysis and Student's t-test were used to compare data. The level of significance was set for p-values <0.05.

3. Results

The first hypothesis explored in this study is whether *L. pneumophila* behaves differently (biofilm colonization and migration), depending on the prevailing mesoscale structure of biofilms shaped by the hydrodynamic conditions. Additionally, the study investigates how biofilm responds to the colonization of *Lp*.

Pf biofilms were formed at 80 RPM, and two different conditions were evaluated, over 24 h, upon *Legionella* spiking: a) the flow regime was kept the same – (80 RPM – 80 RPM) and b) the flow regime was changed to stagnation (80 RPM – Stag).

3.1. Biofilm structural response to L. pneumophila

The mesoscale structure of the pre-established *Pf* biofilms before and 24 h after *Lp* spiking (80 RPM – 80 RPM and 80 RPM – Stag) was evaluated through OCT imaging, as depicted in Fig. 2.

Biofilms kept at 80 RPM appear to be thinner 24 h after *Lp* introduction (comparison Fig. 2a and c). On the other hand, biofilms grown at 80 RPM and then set to stagnation (80 RPM – Stag) become thicker after *Lp* spiking (comparison Fig. 2a and e).

To complement the 2D – OCT images shown in Fig. 2, the 3D – OCT imaging of the biofilms was also accomplished. The videos, corresponding to the reconstruction of 200 2D – OCT stacks, are available in the Supplementary Material (SM) and allow a more detailed investigation of the biofilm mesoscale structure. All the biofilms imaged show an irregular top surface and that the water channels and pores (marked in blue) were essentially positioned in the upper layer of such biofilms. It is also observed that shifting the hydrodynamics from 80 RPM to stagnation (Fig. 2d and e, SM3 video named "80 RPM – Stag, day 4 (24 h after *Lp* spiking)") resulted in the development of biofilms with more protuberances and microcolonies within just 24 h in comparison to the *Pf* biofilm. These biofilms become very similar to the ones found when stagnation was maintained for the entire experiment (Stag – Stag) [14].

The 3D – OCT images were processed in the BISCAP software to determine the mesoscale properties of the biofilm, including biofilm thickness (Fig. 3a) and porosity (Fig. 3b).

When the biofilm is kept under 80 RPM (80 RPM – 80 RPM) the *Lp* spiked biofilms (blue bar) had a significant thickness reduction of ~20 % between days 3 and 4 ($p < 0.0005$). Similarly, there was a significant decrease in biofilm porosity, even though *Legionella* presence aggravated such reduction – from 0.30 ± 0.04 (day 3) to 0.25 ± 0.01 (day 4) for *P. fluorescens* alone and to 0.21 ± 0.01 (day 4, $p < 0.0001$) for the mixed biofilm of *Pf* and *Lp*. Concerning the reincubation of biofilms under stagnation (80 RPM – Stag), the presence of *L. pneumophila* promoted a significant thickness increase between the *Pf* control (19.40 ± 3.09 μm) and the spiked biofilm (45.45 ± 11.11 μm), $p < 0.0001$) in just 24 h. No significant differences were found for porosity. These data are compatible with the OCT observations formerly discussed.

3.2. L. pneumophila migration under different hydrodynamics'

Lp migration within the *Pf* biofilms was followed over 24 h post-spiking using confocal microscopy keeping the 80 RPM dynamic conditions (80 RPM – 80 RPM, Fig. 4) and after a shift from dynamic to stagnant conditions (80 RPM – Stag, Fig. 5). Sampling was performed 5 min, 15 min, 30 min, 45 min and then every 1 h until the 24 h after *Lp* spiking. *Lp* was tracked in red fluorescence using a 16S rRNA PNA-FISH probe.

Confocal images of the *L. pneumophila* positioning and migration across the pre-established *Pf* biofilm, under 80 RPM (condition 80 RPM – 80 RPM), are shown in Fig. 4. *Lp* was observed in the upper layers of the biofilm 5 min after spiking, as indicated by the white arrow in the 3D projection (Fig. 4A) and the predominance of red-fluorescent cells in the orthogonal view (Fig. 4, right box, first line – 5 min). Within 1 h, *Lp* was already distributed between the top and middle layers of the biofilm, with greater accumulation in the later one. This is shown in Fig. 4B, where no *Lp* can be observed at the top of the biofilm through the 3D projection. By the 4-h mark, significant amounts of *Lp* remained in the mid layers of the biofilm, yet some *Lp* began to appear at the bottom, as depicted in the orthogonal view (XZ plane) where the red *Lp* cells appear closer to the bottom – Fig. 4, right box, third line – 4 h. Clear

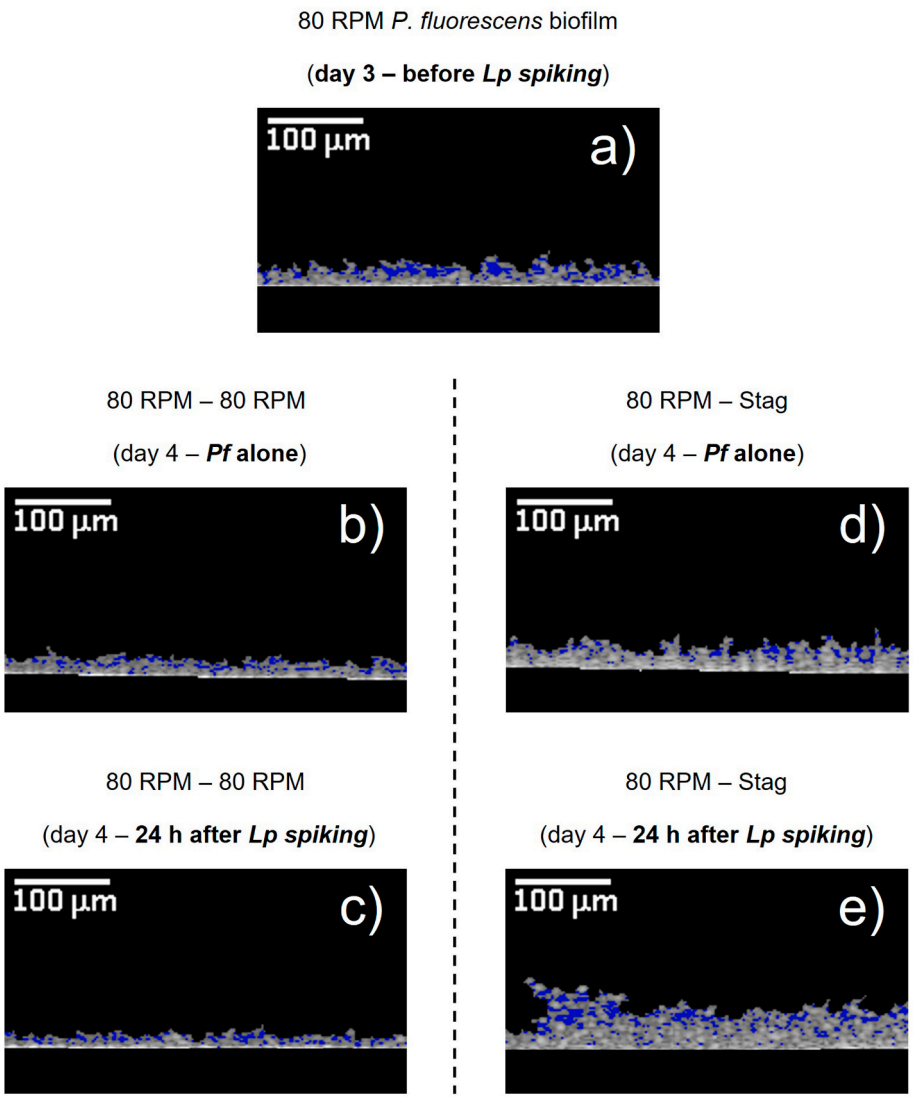

Fig. 2. Representative images obtained by 2D – Optical Coherence Tomography (OCT) of (a) pre-established *P. fluorescens* (*Pf*) biofilms before *L. pneumophila* spiking (on day 3), and *Pf* biofilms (b) alone on day 4 (control) and (c) 24 h after *Lp* spiking under 80 RPM (80 RPM – 80 RPM) – left side, and (d) alone on day 4 (control) and (e) 24 h after *Lp* spiking and reincubation under stagnation (80 RPM – Stag) – right side. The empty spaces within the biofilm structure are coloured blue. (For interpretation of the references to colour in this figure legend, the reader is referred to the Web version of this article.)

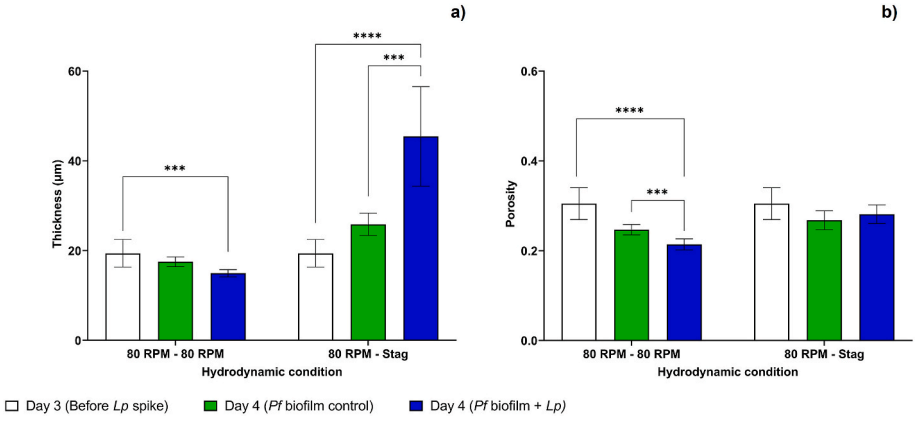

Fig. 3. Thickness (a) and porosity (b) of 80 RPM – 80 RPM and 80 RPM – Stag biofilms before *L. pneumophila* (*Lp)* spiking (day 3, white bars), and on the day after – *P. fluorescens* (*Pf)* biofilm control (day 4, green bars) and *Pf* biofilm spiked with *Lp* (day 4, blue bars). The mean ± standard deviation shown (n = 18) includes three independent experiments with two replicates (coupons) each. Statistically significant differences are represented for $p < 0.0005$ by *** and <0.0001 by ****. The parameters were quantified through the analysis of 3D – OCT images with BISCAP software. (For interpretation of the references to colour in this figure legend, the reader is referred to the Web version of this article.)

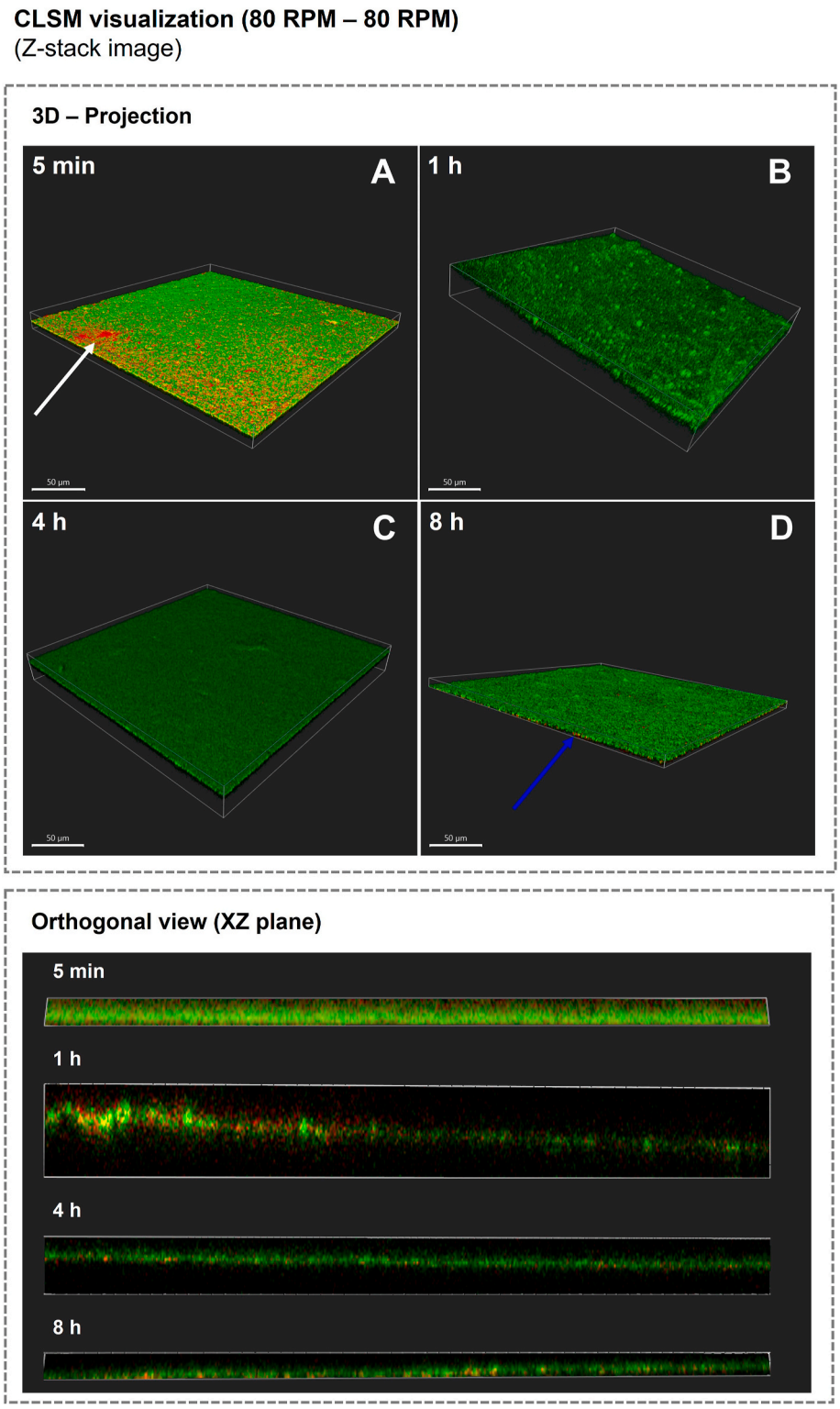

Fig. 4. Representative CLSM images of biofilms 5 min, 1, 4 and 8 h after spiking with *L. pneumophila* under continuous dynamic conditions (80 RPM – 80 RPM). *Lp* was stained with a 16S rRNA PNA probe (in red). The confocal images are 3D projections (left box) and orthogonal XZ planes (right box) of the acquired CLSM images using IMARIS. The white arrow indicates *Lp* presence in the top layer of the biofilm and the blue arrow indicates *Lp* accumulation at the bottom of the biofilm. The white scale bars are 50 µm. (For interpretation of the references to colour in this figure legend, the reader is referred to the Web version of this article.)

accumulation at the bottom was observed 8 h after spiking, and no *Legionella* was found in the top or middle layers (Fig. 4D – the 3D projection demonstrate two distinct layers). These results suggest that *Lp* had an initial preference for the middle of the biofilm before reaching the bottom.

Lp migration pattern within the *Pf* biofilm at stagnation (80 RPM – Stag) - Fig. 5 - is different than the one previously discussed. *L. pneumophila* was detected in the top of the biofilm within the first 5 min after spiking (Fig. 5A, red cells accumulated in the top of the XZ orthogonal view – right box, first line). The orthogonal views

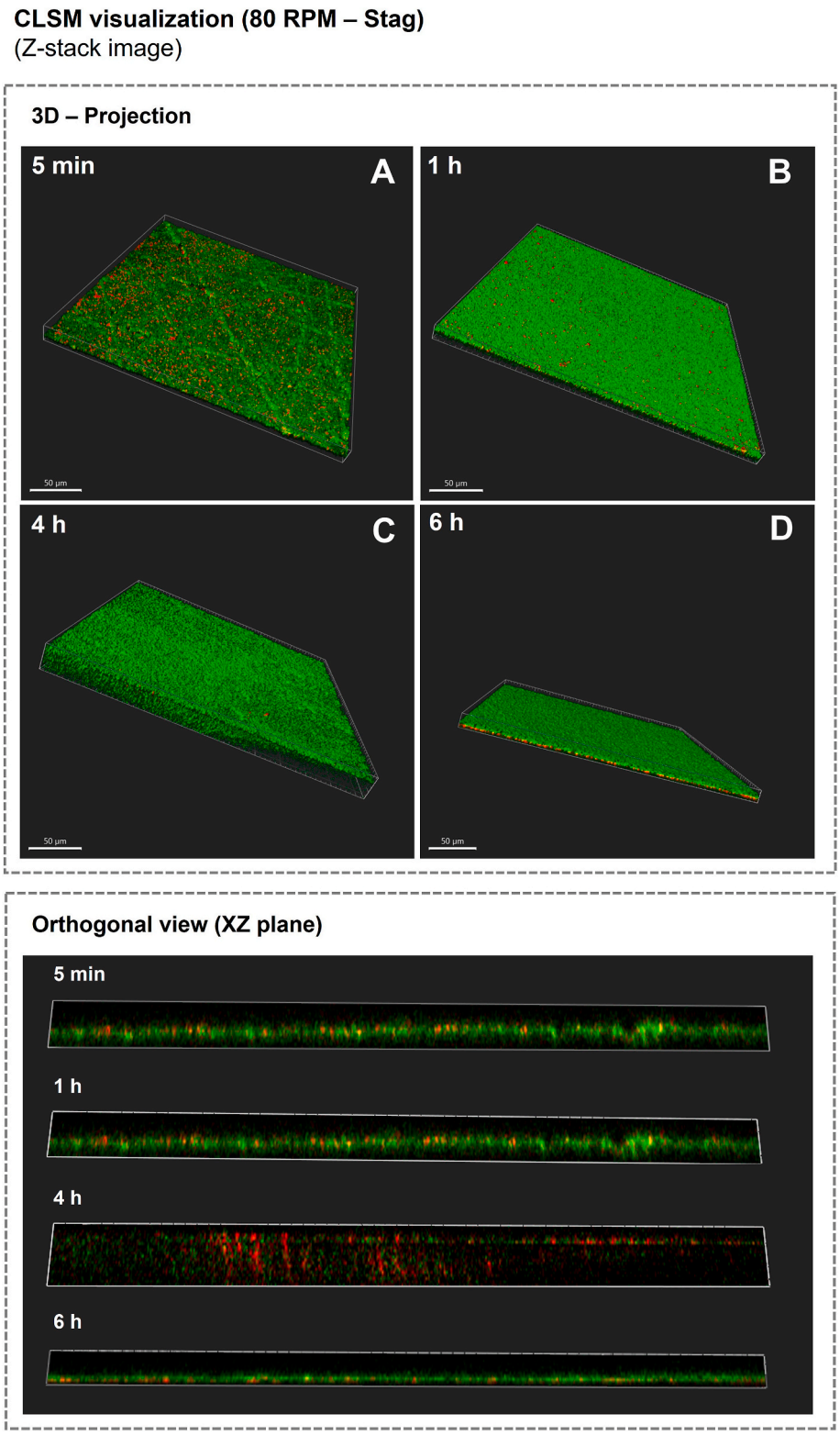

Fig. 5. Representative CLSM images of biofilms 5 min, 1, 4 and 6 h after spiking with *L. pneumophila* (*Lp*) under continuous dynamic conditions (80 RPM – 80 RPM). *Lp* was stained with a 16S rRNA PNA probe (in red). The confocal images are 3D projections and orthogonal XZ planes of the acquired CLSM images using IMARIS. The white scale bars are 50 µm. (For interpretation of the references to colour in this figure legend, the reader is referred to the Web version of this article.)

corresponding to the time points of 1 and 4 h (Fig. 5, right box, second and third line) show a progressive movement of *Lp* across the biofilm. For instance, at the 4-h mark, *Lp* seems to start reaching the bottom (Fig. 5 – right box, third line). Finally, as can be observed through the two distinct layers of bacteria (both in the 3D projection – Fig. 5D – and the orthogonal view), 6 h after the spiking, *Lp* is mostly located at the bottom of the biofilm. The migration was faster than under continuous dynamic conditions (80 RPM-80 RPM).

The biovolume of *Pf* and *Lp* were determined 24 h after spiking and the ratio of *Pf* over *Lp* is presented in Fig. 6.

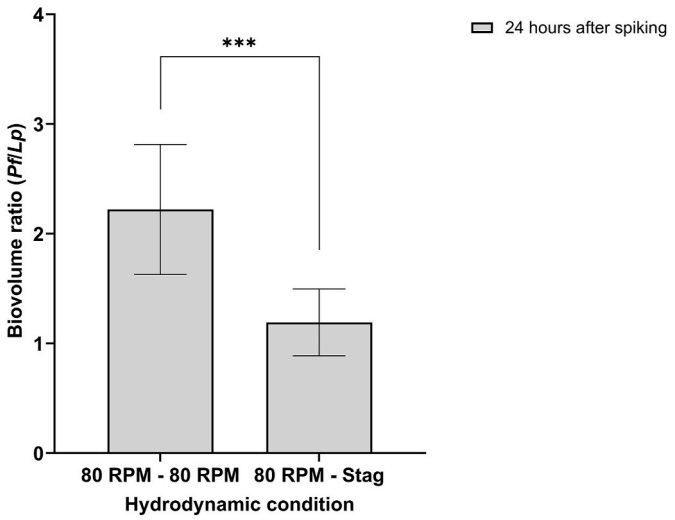

Fig. 6. The ratio of the biovolumes of *P. fluorescens* (*Pf*) and *L. pneumophila* (*Lp*) in spiked biofilms 24 h after spiking with hydrodynamic conditions set to 80 RPM (80 RPM – 80 RPM) and to stagnation (80 RPM – Stag). The biovolume values were extracted from confocal microscopy images with the COMSTAT plugin. The mean ± standard deviation (n = 18) shown includes three independent experiments with two replicates (coupons) each. Statistically significant differences are represented for $p < 0.0005$ by ***.

The biovolume data is presented as the ratio between the biovolume of *Pf* and *Lp*. The biovolume ratio significantly decreases when stagnation is imposed on the biofilms ($p < 0.0005$).

3.3. *L. pneumophila* behavior within biofilms over time

One of the most important physiological characteristics of *Legionella* is its ability to enter the VBNC state [43]. Fig. 7 shows *L. pneumophila* culturability (colony-forming units, blue line), PNA-positive cells (PNA-FISH assay, black line), and VBNC cells (DVC-FISH assay, expressed as percentage values) data over 11 days in biofilms (corresponding to a biofilm with 14 days) under the 80 RPM–80 RPM (Figs. 7a) and 80 RPM – Stag (Fig. 7b) conditions.

Fig. 7 shows that very high numbers of PNA-positive *Lp* cells (black lines) were observed over the 11 days of *Lp* residence within the biofilm, regardless of the tested conditions ($p > 0.01$). Also, the constant *Lp* cell numbers over time reveal that cells enter very quickly in a pseudo-steady state.

Regarding the culturable *Lp* numbers, significant differences were found between days 4 and 7 for the 80 RPM – Stag biofilms, as the cultivability decreased (4.61 ± 0.12 to 3.56 ± 0.27 $\log_{10}$CFU/cm^2, $p <$ 0.0001). However, from days 7–14, the *Lp* cultivable numbers remained constant. Regarding the 80 RPM – 80 RPM condition, no significant differences were found in *Legionella* culturability until day 9. Afterwards, *Lp* stopped being recovered from the 80 RPM – 80 RPM biofilms, while in the 80 RPM – Stag it was culture recovered until day 14. That was an earlier indicator that the continuous dynamic conditions could induce *Lp* into VBNC earlier than when stagnation is imposed after spiking. That hypothesis was confirmed by the different VBNC percentages on days 11 and 14 (93 and 94 % vs 58 and 60 %, respectively). Furthermore, there were no significant differences ($p > 0.01$) between both hydrodynamic conditions until day 9.

It is important to highlight that in both hydrodynamic conditions the numbers of PNA-positive *Lp* cells (FISH-assay, black line) were significantly higher ($p < 0.0001$) than the numbers of cultivable cells (blue line). Surprisingly, just after 24 h in the biofilm, 43 % of the *L. pneumophila* population is already in VBNC. Nevertheless, the real number of viable cells might be underestimated, as the DVC method used R2 nutrient medium (in line with some reported studies) instead of BCYE. Since this method relies on cell elongation – indicative of cell division – it may not capture all viable cells accurately [44]. Moreover, given the preference of *Legionella* for BCYE, it is possible that the cells would be more likely to divide, potentially resulting in a higher number of elongated cells.

4. Discussion

The results show that hydrodynamics' play a crucial role in how biofilm and *Legionella* interact. Changing from 80 RPM to stagnation, compared to maintaining 80 RPM throughout the experiment, results in (a) a significant increase in biofilm thickness, (b) accelerated migration of *Legionella* to the bottom of the biofilm, and (c) a decreased concentration of culturable *L. pneumophila* (VBNC) within the biofilm.

Additionally, the presence of water channels within the biofilm seems to be a facilitating aspect for *L. pneumophila* migration. To further support the discussion, key findings from this study are summarized in Table 1. It also includes data from a previous study accomplished by the same authors [14], where *Pf* biofilm and *Lp* colonization were conducted under stagnation for the entire experimental period.

4.1. *Biofilm structural rearrangement upon Legionella colonization, shaped by hydrodynamics*

The structural shifts of biofilms in response to pathogen colonization are well-documented in the literature [14,45]. Biofilm structures tend to rearrange in a way that dominant bacteria within the consortium can meet their nutritional and physiological needs while maintaining their dominance [46]. This phenomenon, along with the physiological requirements of *Legionella* [47,48] appears to drive the readjustments of *Pf*

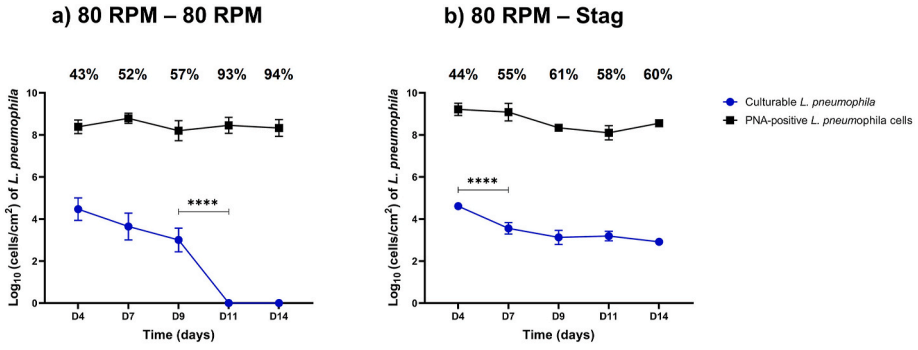

Fig. 7. The number of culturable (CFU, $\log_{10}$ CFU/cm^2 or mL) and PNA-positive cell counts of *L. pneumophila* (*Lp*; cells/cm^2) over time for (a) 80 RPM – 80 RPM and (b) 80 RPM – Stag biofilms. The percentages of the *Lp* population in VBNC are shown for each timepoint and were calculated considering the culturable and the total *Lp* cell counts. The mean ± standard deviation (n = 12 for the culturable cells and n = 120 for the PNA-positive cell counts) shown includes three independent experiments with two replicates (coupons) each. Statistically significant differences are represented for $p < 0.0005$ by *** and <0.0001 by ****.

Table 1
Data regarding L. *pneumophila* migration within differently structured biofilms.

Hydrodynamic condition	Time to reach the layer			Linear migration velocity to the bottom[b]	Biofilm structural parameters[c]				Biovolume ratio (Pf/Lp)	Culturable Pf in the biofilm (log10 CFU/cm2)	
	Top	Middle	Bottom		Biofilm thickness		Biofilm porosity				
					Before *Lp*	24 h after *Lp*	Before *Lp*	24 h after *Lp*		Before *Lp*	24 h after *Lp*
80 RPM – 80 RPM	5–15 min	30 min-1 hour	6–8 h	≈2 μm/h	19 μm	15 μm	0.30	0.21	2.22	7.7	6.9
80 RPM – Stag	5–15 min	1–2 h	4–6 h	≈6 μm/h		45 μm		0.28	1.19		7.0
Stag - Stag[a]	15–30 min	1–2 h	2–4 h	≈22 μm/h	57 μm	56 μm	0.19	0.23	1.0	7.4	7.5

[a] Data were collected from Ref. [14] and correspond to biofilms grown under stagnation before and after *Lp* spike.
[b] Calculated considering the average thickness of the biofilm before and after *Lp* spiking and the average time to reach the bottom.
[c] The presented parameters correspond to the quantitative analysis made to the OCT images.

observed in this study. So, the primary biofilm producer and initial colonizer, *Pseudomonas,* defines the dominant biofilm structure, allowing *Legionella* to use existing pores and water channels for rapid migration to the biofilm's bottom [14].

Interestingly, biofilm rearrangements are different according to the hydrodynamic conditions imposed after *Lp* spiking. For instance, maintaining 80 RPM throughout the experiment (80 RPM – 80 RPM) causes *Legionella* to destabilize the upper layers of the biofilm (SM1 and SM2, "80 RPM, day 3 (before *Lp* spiking)" and 80 RPM – 80 RPM, day 4 (24 h after *Lp* spiking)"), leading to sloughing-off and thickness reduction [49]. Given that most pores and water channels in the initial *Pf* biofilm are in the upper layers (SM1, "80 RPM, day 3 (before *Lp* spiking)"), it is not surprising that biofilm removal results in decreased porosity. These findings agree with those of Puga et al. (2016), who observed that spiking *L. monocytogenes* into pre-established *P. fluorescens* biofilms at 80 RPM resulted in diminished thickness and increased compaction [45]. The authors hypothesized that species interactions led to the production of new extracellular matrix components, causing matrix reduction.

Similarly, in our study, biofilm thickness significantly increased under stagnation, indicating an overproduction of biomass in response to *L. pneumophila* entry. Dong et al. (2023) reported similar findings, noting that *Enterococcus faecalis* biofilms became thicker when pathogens such as *Escherichia coli* O157:H7 and *Salmonella enteritidis* were introduced into the microbial consortium [46]. It has been suggested that *E. faecalis* manipulates the microenvironment through structural changes and the activation of "biological weapons". Silva et al. (2024) reached similar conclusions [14].

However, it is noteworthy that when stagnation is maintained throughout the experiment (during biofilm build-up and spiking), *P. fluorescens* biofilms take several days post-*L. pneumophila* colonization to increase thickness. As summarized in Table 1 (Stag – Stag condition), no significant thickness changes were observed 24 h after spiking. The rapid rearrangement of the *Pf* biofilms (80 RPM – Stag) is likely linked to the cessation of shear forces. *Pf* capitalizes on the accumulation of suspended solids within the biofilm, also benefiting from the absence of removal forces [50].

Increased fluid velocity enhances turbulence near the biofilm surface, improving mass transfer between the bulk fluid and the biofilm, which facilitates the exchange of oxygen, nutrients, and metabolic waste [29,51]. Simultaneously, biofilm experiences shear forces, resulting in increased removal rates that likely justify the reduced thickness at 80 RPM in comparison to the one at stagnation [52,53].

The interplay between biofilm structure, flow regime, and *Legionella* interaction has been previously acknowledged. For example, Shen et al. (2015) demonstrated that local flow hydrodynamics affect biofilm roughness, altering the biofilm surface area and consequently influencing *Legionella* adhesion [11].

4.2. *Legionella* migration across the biofilm: biofilm structure and hydrodynamics

Legionella migration patterns within biofilms varied significantly depending on the hydrodynamic conditions imposed during biofilm formation and the ones after spiking. *Legionella* exhibits flagellar motility, which further supports its ability to navigate through biofilms [54]. Nonetheless, as summarized in Table 1, regardless of the tested conditions, *Lp* was entirely located in the bottom layers of the biofilms within less than 8 h after spiking. A key driver for *Legionella* movement to the bottom of the biofilm is its microaerophilic nature, which allows it to thrive in environments with lower oxygen availability [47]. The bottom layers, while having lower oxygen levels, will favour *Legionella* physiological requirements [47].

Not surprisingly, the structure of the biofilms seems to be important to how fast *Legionella* reaches the bottom layers of the biofilm. A first insight from the results is that biofilm porosity is probably closely related to *Legionella* migration. Biofilms formed at 80 RPM and set to stagnation (80 RPM – Stag) kept the same porosity over the 24 h after *Lp* spiking (Table 1), enabling a faster movement of *Legionella* across the biofilm. Indeed, as shown in the videos (SM3), the water-filled structures within the biofilm are mostly positioned at the biofilm top layers keeping the environment near the surface with higher oxygen content leading *Lp* to migrate away from this region. However, it is important to note that, while porosity is the same, biofilm thickness increased over time meaning that new water-filled structures have been established, probably as a result of *Legionella* movement across the biofilm structure. For instance, Houry et al. (2012) reported that a strain of *B. thuringiensis* swims over the biofilm matrix and rapidly reaches the bottom by creating channels [55]. The rearrangement into a thicker structure undergone over the 24 h period is the most likely reason why the migration velocity observed for the 80 RPM – Stag condition is substantially lower than the one observed when stagnation (Stag – Stag) was kept for the entire experiment [55].

Additionally, the CLSM images show that when the experiment ran the whole period under shear (80 RPM – 80 RPM), *Lp* accumulated during some hours in the middle layers. The videos in the supplementary material clearly show that at 80 RPM the water-filled areas (marked in blue) are evenly distributed across the biofilm height (SM2). This promotes an increased oxygen concentration at the bottom of the biofilm, diminishing the driving force that pushes *Legionella* to the bottom.

Another hypothesis to justify the different migration rates across the distinct studied conditions is related to the bacterial species biovolume. A higher *Pf/Lp* biovolume ratio was observed for the lower migration rate, even though there are no significant differences for culturable *Pf* (last two columns, Table 1). The higher volumetric densities of *Pf* cells in comparison with the one from *Lp* (80 RPM – 80 RPM), are expected to restrict *Lp* movement across the biofilm not only due to space constrains [55], but also due to relative abundance of the dominant bacterial

species.

Apart from the time *Legionella* needs to reach the bottom layers, it is important to remark that under stagnation, and facing the sedimentation forces, *Legionella* needed between 15 and 30 min to be detected at the top of the biofilm. While it was much faster (between 5 min and 15 min) to reach the top of the biofilms formed under 80 RPM, regardless of the hydrodynamics imposed after spiking. As mentioned, Shen et al. (2015) observed a positive correlation between the biofilm roughness, which increases the surface area, and *L. pneumophila* adhesion to biofilms [11]. In the present study 80 RPM-grown biofilms were rougher (data not shown) than the ones grown under stagnation (data not shown), which might explain the quickest adhesion of *L. pneumophila* to the biofilm top layer. Finally, in the migration under 80 RPM, it is feasible to accept that shear forces prevail over the Brownian motion [51,56], which drives *Legionella* into flow-driven paths to the top of the biofilm. Under stagnation, it is likely that Brownian motion and flagellar motility are more relevant regarding *Legionella* migration to overcome the effects of sedimentation [17,57,58]. *Legionella*'s movement within the biofilm is likely influenced by chemotaxis [59], driven by its need for nutrients like cysteine and iron, and lower oxygen/redox conditions. In dynamic environments, where lower oxygen zones are less prevalent, *Legionella* takes longer to reach the bottom of the biofilm, despite its preference for those regions.

4.3. *Legionella behaviour within the biofilm: how fast does it enter the VBNC state?*

A significant portion of the *L. pneumophila* population (~45 %) is in VBNC state, in just 24 h. This can be partially explained by the fact that culture methods underestimate *Legionella* cultivable numbers [60,61]. Even the samples' pre-treatment with acid or heat treatment (as accomplished in the present study) were shown to increase underestimation [8]. The transition of *Lp* to the VBNC state is a survival strategy of the bacteria triggered by environmental stresses. In this state, *Legionella* remains metabolically active but loses the ability to form colonies on standard culture media [62]. In the present study, *Legionella* is under nutritional stress since none of the nutritional requirements for its growth is supplied. However, findings are similar to other studies that showed that a stable sub-population of *Legionella* in VBNC resisted for several months under starvation [63]. Nisar et al. (2024) reported that almost half of the *Legionella* population in a biofilm (with a diverse community of bacteria and amoebae) grown in a model plumbing system was in the VBNC state, with this sub-population demonstrating high tolerance to environmental stresses such as nutrient depletion and chlorine exposure [64]. Additionally, *Pf* is known to support *Legionella* settlement but not its growth [34]. Both aspects might have triggered the quick *Legionella* shift to VBNC.

More intriguing is *L. pneumophila*'s "choice" to colonize the biofilm. Entering the biofilm seems to speed up culturability loss in comparison to what happens in the bulk, where only 17 % of the *L. pneumophila* population entered VBNC (data not shown). So, why did *Legionella* enter the biofilms? One hypothesis that has been already discussed concerns the effect of gravity (sedimentation). In that case, the energy spent by bacteria to keep swimming in the bulk would be extremely high in comparison to the one spent at the biofilm. Additionally, under the stress conditions imposed in the current study, entering the biofilm is arguably a long-term more successful survival strategy. In the absence of key nutrients in the bulk, the biofilm provides protection against external aggression [65,66] and allows *Legionella* to persist under a more favourable microaerophilic environment [47]. Concerning the two tested conditions, under shear (80 RPM – 80 RPM) *Lp* lost culturability faster than when set to stagnation. Probably, this difference is related to the shear forces and lower biofilm thicknesses (higher oxygen concentration) promoting an increased stress for *Legionella*.

It is worth highlighting the high number of total viable cells (~log8) observed over the 11 days of the experiment. No significant decrease ($p > 0.05$) was observed over time in cells' viability regardless of the decrease in cells' culturability. This suggests that an extremely high number of cells can replicate as soon as the conditions become favourable. This, associated with the fact that *Legionella* is positioned at the bottom of the biofilm, raises serious concerns for *Legionella* monitoring and control practices in water systems. Most *Legionella* monitoring approaches in real field systems are grounded on culture-based water sampling, disregarding the role of biofilms. Given that, if the data from the present work would refer to a real field scenario, most certainly *Legionella* risk would be underestimated (low numbers of CFU's).

Apart from the scientific questions addressed in the current investigation, there is a final contribution associated with the combination of imaging methods for biofilm studies which can strengthen the current real-field studies concerning *Legionella*. Finally, the authors recognize that the platform of study does not represent the interactions of biofilms and *Legionella* in engineered water systems. Yet, it allows the approach of several questions regarding *Legionella*-biofilms interactions.

5. Conclusions

Understanding the interactions between *Legionella* and biofilms concerning hydrodynamic conditions is vital for advancing biofilm analysis and monitoring. In the present study, a biofilm model of *P. fluorescens* grown in 12-well plates was used. This investigation's main conclusions are:

(i) Stagnation significantly increases the risk of *Legionella* proliferation, as thicker biofilms facilitate faster colonization and settlement of the bacteria at the biofilms' bottom.
(ii) The water channels within biofilms seem to be crucial in enabling *Legionella* movement throughout the biofilm structure.
(iii) While high concentrations of viable *L. pneumophila* cells remain constant for 11 days, exposure to shear conditions leads to a complete loss of culturability after 9 days, resulting in 100 % of the population entering the viable but nonculturable (VBNC) state.

CRediT authorship contribution statement

Ana Rosa Silva: Writing – review & editing, Writing – original draft, Visualization, Methodology, Investigation, Formal analysis, Data curation, Conceptualization. **C. William Keevil:** Writing – review & editing, Supervision, Methodology, Conceptualization. **Ana Pereira:** Writing – review & editing, Writing – original draft, Supervision, Resources, Methodology, Funding acquisition, Conceptualization.

Data availability

Data will be made available on request to the corresponding author.

Declaration of competing interest

The authors have no competing interests to declare.

Acknowledgments

This work was financially supported by national funds through FCT/MCTES (PIDDAC): LEPABE, UIDB/00511/2020 (DOI: 10.54499/UIDB/00511/2020) and UIDP/00511/2020 (DOI: 10.54499/UIDP/00511/2020) and ALiCE, LA/P/0045/2020 (DOI: 10.54499/LA/P/0045/2020); by national funds through the FCT/MCTES (PIDDAC), under the project 2022.03523.PTDC - LegioFilms - Understanding the Role of Biofilm Architecture in *Legionella* Colonization and Risk of Detachment in hospital networks using an Integrated Monitoring Approach, with DOI 10.54499/2022.03523.PTDC (https://doi.org/10.54499/2022.03523.PTDC). Ana Rosa Silva thanks the Portuguese Foundation for Science

and Technology (FCT) for the financial support of the PhD grant (2020.08539.BD).

Appendix A. Supplementary data

Supplementary data to this article can be found online at https://doi.org/10.1016/j.bioflm.2025.100258.

References

[1] Pereira A, Silva AR, Melo LF. *Legionella* and biofilms—integrated surveillance to bridge science and real-field demands. Microorganisms 2021;9:1212. https://doi.org/10.3390/microorganisms9061212.

[2] Margot C, Rhoads W, Gabrielli M, Olive M, Hammes F. Dynamics of drinking water biofilm formation associated with *Legionella* spp. Colonization. npj Biofilms Microbiomes 2024;10:101. https://doi.org/10.1038/s41522-024-00573-x.

[3] Walker JT. The influence of climate change on waterborne disease and *Legionella*: a review. Perspect Pub Health 2018;138:282–6. https://doi.org/10.1177/1757913918791198.

[4] Kirschner AKT. Determination of viable legionellae in engineered water systems: do we find what we are looking for? Water Res 2016;93:276–88. https://doi.org/10.1016/j.watres.2016.02.016.

[5] Almonacid Garrido MC, Villanueva-Suárez MJ, Montes Martín MJ, Garcia-Alonso A, Tenorio Sanz MD. Prevalence and distribution of *Legionella* in municipal drinking water supply systems in Madrid (Spain) and risk factors associated. Sci Total Environ 2024;954:176655. https://doi.org/10.1016/j.scitotenv.2024.176655.

[6] Voulvoulis N. Water reuse from a circular economy perspective and potential risks from an unregulated approach. Curr Opin Env Sci Hl 2018;2:32–45. https://doi.org/10.1016/j.coesh.2018.01.005.

[7] Kanarek P, Bogiel T, Breza-Boruta B. Legionellosis risk—an overview of *Legionella* spp. Habitats in europe. Environ Sci Pollut Res 2022;29:76532–42. https://doi.org/10.1007/s11356-022-22950-9.

[8] Nisar MA, Ross KE, Brown MH, Bentham R, Best G, Whiley H. Detection and quantification of viable but non-culturable *Legionella pneumophila* from water samples using flow cytometry-cell sorting and quantitative PCR. Front Microbiol 2023;14:1094877. https://doi.org/10.3389/fmicb.2023.1094877.

[9] Pierre D, Baron JL, Ma X, Sidari FP, Wagener MM, Stout JE. Water quality as a predictor of *Legionella* positivity of building water systems. Pathogens 2019;8:295. https://doi.org/10.3390/pathogens8040295.

[10] Nisar MA, Ross KE, Brown MH, Bentham R, Whiley H. *Legionella pneumophila* and Protozoan hosts: implications for the control of hospital and potable water systems. Pathogens 2020;9:286. https://doi.org/10.3390/pathogens9040286.

[11] Shen Y, Monroy GL, Derlon N, Janjaroen D, Huang C, Morgenroth E, Boppart SA, Ashbolt NJ, Liu W-T, Nguyen TH. Role of biofilm roughness and hydrodynamic conditions in *Legionella pneumophila* adhesion to and detachment from simulated drinking water biofilms. Environ Sci Technol 2015;49:4274–82. https://doi.org/10.1021/es505842v.

[12] Nisar MA, Ross KE, Brown MH, Bentham R, Hinds J, Whiley H. Molecular screening and characterization of *Legionella pneumophila* associated free-living amoebae in domestic and hospital water systems. Water Res 2022;226:119238. https://doi.org/10.1016/j.watres.2022.119238.

[13] Nisar MA, Ross KE, Brown MH, Bentham R, Whiley H. Water stagnation and flow obstruction reduces the quality of potable water and increases the risk of legionelloses. Front Environ Sci 2020;8. https://doi.org/10.3389/fenvs.2020.611611.

[14] Silva AR, Melo LF, Keevil CW, Pereira A. *Legionella* colonization and 3D spatial location within a *Pseudomonas* biofilm. Sci Rep 2024;14:16781. https://doi.org/10.1038/s41598-024-67712-4.

[15] Shaheen M, Ashbolt NJ. Differential bacterial predation by free-living amoebae may result in blooms of *Legionella* in drinking water systems. Microorganisms 2021;9:174. https://doi.org/10.3390/microorganisms9010174.

[16] Paniagua AT, Paranjape K, Hu M, Bédard E, Faucher SP. Impact of temperature on *Legionella pneumophila*, its Protozoan host cells, and the microbial diversity of the biofilm community of a pilot cooling tower. Sci Total Environ 2020;712:136131. https://doi.org/10.1016/j.scitotenv.2019.136131.

[17] Barbosa A, Azevedo NF, Goeres DM, Cerqueira L. Ecology of *Legionella pneumophila* biofilms: the link between transcriptional activity and the biphasic cycle. Biofilms 2024;7:100196. https://doi.org/10.1016/j.bioflm.2024.100196.

[18] Soares A, Gomes LC, Monteiro GA, Mergulhão FJ. Hydrodynamic effects on biofilm development and recombinant protein expression. Microorganisms 2022;10:931. https://doi.org/10.3390/microorganisms10050931.

[19] Araújo PA, Malheiro J, Machado I, Mergulhão F, Melo L, Simões M. Influence of flow velocity on the characteristics of *Pseudomonas fluorescens* biofilms. J Environ Eng 2016;142:4016031. https://doi.org/10.1061/(ASCE)EE.1943-7870.0001068.

[20] Ji P, Rhoads WJ, Edwards MA, Pruden A. Impact of water heater temperature setting and water use frequency on the building plumbing microbiome. ISME J 2017;11:1318–30. https://doi.org/10.1038/ismej.2017.14.

[21] Tsagkari E, Connelly S, Liu Z, McBride A, Sloan WT. The role of shear dynamics in biofilm formation. NPJ Biofilms Microbiomes 2022;8:33. https://doi.org/10.1038/s41522-022-00300-4.

[22] Melo LF, Vieira MJ. Physical stability and biological activity of biofilms under turbulent flow and low substrate concentration. Bioprocess Eng 1999;20:363–8. https://doi.org/10.1007/s004490050604.

[23] van Loosdrecht MCM, Heijnen JJ, Eberl H, Kreft J, Picioreanu C. Mathematical modelling of biofilm structures. Antonie Leeuwenhoek 2002;81:245–56. https://doi.org/10.1023/A:1020527020464.

[24] Huang CK, Weerasekara A, Lu J, Carter R, Weynberg KD, Thomson R, Bell S, Guo J. Extended water stagnation in buildings during the COVID-19 pandemic increases the risks posed by opportunistic pathogens. Water Res X 2023;21:100201. https://doi.org/10.1016/j.wroa.2023.100201.

[25] De Giglio O, Diella G, Lopuzzo M, Triggiano F, Calia C, Pousis C, Fasano F, Caggiano G, Calabrese G, Rafaschieri V, et al. Impact of lockdown on the microbiological status of the hospital water network during COVID-19 pandemic. Environ Res 2020;191:110231. https://doi.org/10.1016/j.envres.2020.110231.

[26] Cavallaro A, Rhoads WJ, Sylvestre É, Marti T, Walser J-C, Hammes F. *Legionella* relative abundance in shower hose biofilms is associated with specific microbiome members. FEMS Microbes 2023;4:xtad016. https://doi.org/10.1093/femsmc/xtad016.

[27] Taylor M, Ross K, Bentham R. Spatial arrangement of *Legionella* colonies in intact biofilms from a model cooling water system. Microbiol Insights 2013;6:49–57. https://doi.org/10.4137/MBI.S12196.

[28] Wang H, Bédard E, Prévost M, Camper AK, Hill VR, Pruden A. Methodological approaches for monitoring opportunistic pathogens in premise plumbing: a review. Water Res 2017;117:68–86. https://doi.org/10.1016/j.watres.2017.03.046.

[29] Gloag ES, Fabbri S, Wozniak DJ, Stoodley P. Biofilm mechanics: implications in infection and survival. Biofilms 2020;2:100017. https://doi.org/10.1016/j.bioflm.2019.100017.

[30] Donlan RM. Biofilms: microbial life on surfaces. Emerg Infect Dis 2002;8:881–90. https://doi.org/10.3201/eid0809.020063.

[31] Flemming H-C, van Hullebusch ED, Neu TR, Nielsen PH, Seviour T, Stoodley P, Wingender J, Wuertz S. The biofilm matrix: multitasking in a shared space. Nat Rev Microbiol 2023;21:70–86. https://doi.org/10.1038/s41579-022-00791-0.

[32] Charlton SGV, Jana S, Chen J. Yielding behaviour of chemically treated *Pseudomonas fluorescens* biofilms. Biofilms 2024;8:100209. https://doi.org/10.1016/j.bioflm.2024.100209.

[33] Wagner M, Horn H. Optical coherence Tomography in biofilm research: a comprehensive review. Biotechnol Bioeng 2017;114:1386–402. https://doi.org/10.1002/bit.26283.

[34] Stewart CR, Muthye V, Cianciotto NP. *Legionella pneumophila* persists within biofilms formed by *Klebsiella pneumoniae, flavobacterium* sp., and *Pseudomonas fluorescens* under dynamic flow conditions. PLoS One 2012;7:1–8. https://doi.org/10.1371/journal.pone.0050560.

[35] Silva AR, Narciso DAC, Gomes LC, Martins FG, Melo LF, Pereira A. Proof-of-Concept approach to assess the impact of thermal disinfection on biofilm structure in hot water networks. J Water Process Eng 2023;53:103595. https://doi.org/10.1016/j.jwpe.2023.103595.

[36] Romeu MJ, Miranda JM, de Jong ED, Morais J, Vasconcelos V, Sjollema J, Mergulhão FJ. Understanding the flow behavior around marine biofilms. Biofilms 2024;7:100204. https://doi.org/10.1016/j.bioflm.2024.100204.

[37] Narciso DAC, Pereira A, Dias NO, Melo LF, Martins FG. Characterization of biofilm structure and properties via processing of 2D optical coherence Tomography images in BISCAP. Bioinformatics 2022;38:1708–15. https://doi.org/10.1093/bioinformatics/btac002.

[38] Narciso DAC, Pereira A, Dias NO, Monteiro M, Melo LF, Martins FG. 3D optical coherence Tomography image processing in BISCAP: characterization of biofilm structure and properties. Bioinformatics 2024;40:btae041. https://doi.org/10.1093/bioinformatics/btae041.

[39] Wilks SA, Keevil CW. Suitability of peptide nucleic acid probes for detection of *Legionella* in mains drinking water supplies. Legionella: State of the Art 30 Years after Its Recognition 2006:442–5. https://doi.org/10.1128/9781555815660.ch105.

[40] Meyer JM, Abdallah MA. The fluorescent pigment of *Pseudomonas fluorescens*: biosynthesis, purification and physicochemical properties. Microbiology 1978;107:319–28. https://doi.org/10.1099/00221287-107-2-319.

[41] Wilks SA, Keevil CW. Targeting species-specific low-affinity 16S RRNA binding sites by using peptide nucleic acids for detection of legionellae in biofilms. Appl Environ Microbiol 2006;72:5453–62. https://doi.org/10.1128/AEM.02918-05.

[42] Juhna T, Birzniece D, Larsson S, Zulenkovs D, Sharipo A, Azevedo NF, Ménard-Szczebara F, Castagnet S, Féliers C, Keevil CW. Detection of *Escherichia coli* in biofilms from pipe samples and coupons in drinking water distribution networks. Appl Environ Microbiol 2007;73:7456–64. https://doi.org/10.1128/AEM.00845-07.

[43] Epalle T, Girardot F, Allegra S, Maurice-Blanc C, Garraud O, Riffard S. Viable but not culturable forms of *Legionella pneumophila* generated after heat shock treatment are infectious for macrophage-like and alveolar epithelial cells after resuscitation on acanthamoeba polyphaga. Microb Ecol 2015;69:215–24. https://doi.org/10.1007/s00248-014-0470-x.

[44] Kumar SS, Ghosh AR. Assessment of bacterial viability: a comprehensive review on recent advances and challenges. Microbiology 2019;165:593–610. https://doi.org/10.1099/mic.0.000786.

[45] Puga CH, Orgaz B, SanJose C. *Listeria monocytogenes* impact on mature or old *Pseudomonas fluorescens* biofilms during growth at 4 and 20°C. Front Microbiol 2016;7. https://doi.org/10.3389/fmicb.2016.00134.

[46] Jiajun D, Luhan L, Liying C, Yuqiang X, Yabin W, Youbao Z. The coexistence of bacterial species restructures biofilm architecture and increases tolerance to

antimicrobial agents. Microbiol Spectr 2023;11:e03581. https://doi.org/10.1128/spectrum.03581-22. 22.
[47] Mauchline WS, Keevil CW. Development of the BIOLOG substrate utilization system for identification of *Legionella* spp. Appl Environ Microbiol 1991;57:3345–9. https://doi.org/10.1128/aem.57.11.3345-3349.1991.
[48] Mauchline WS, Araujo R, Wait R, Dowsett AB, Dennis PJ, Keevil CW. Physiology and morphology of *Legionella pneumophila* in continuous culture at low oxygen concentration. Microbiology 1992;138:2371–80. https://doi.org/10.1099/00221287-138-11-2371.
[49] Boles BR, Horswill AR. Agr-mediated dispersal of *Staphylococcus aureus* biofilms. PLoS Pathog 2008;4:e1000052. https://doi.org/10.1371/journal.ppat.1000052.
[50] Carvalho FM, Teixeira-Santos R, Mergulhão FJM, Gomes LC. Effect of *lactobacillus plantarum* biofilms on the adhesion of *Escherichia coli* to urinary tract devices. Antibiotics 2021;10:966. https://doi.org/10.3390/antibiotics10080966.
[51] Krsmanovic M, Biswas D, Ali H, Kumar A, Ghosh R, Dickerson AK. Hydrodynamics and surface properties influence biofilm proliferation. Adv Colloid Interface Sci 2021;288:102336. https://doi.org/10.1016/j.cis.2020.102336.
[52] Tsagkari E, Sloan WT. Turbulence accelerates the growth of drinking water biofilms. Bioproc Biosyst Eng 2018;41:757–70. https://doi.org/10.1007/s00449-018-1909-0.
[53] Paul E, Ochoa JC, Pechaud Y, Liu Y, Liné A. Effect of shear stress and growth conditions on detachment and physical properties of biofilms. Water Res 2012;46:5499–508. https://doi.org/10.1016/j.watres.2012.07.029.
[54] Lau HY, Ashbolt NJ. The role of biofilms and Protozoa in *Legionella* pathogenesis: implications for drinking water. J Appl Microbiol 2009;107:368–78. https://doi.org/10.1111/j.1365-2672.2009.04208.x.
[55] Houry A, Gohar M, Deschamps J, Tischenko E, Aymerich S, Gruss A, Briandet R. Bacterial swimmers that infiltrate and take over the biofilm matrix. Proc Natl Acad Sci USA 2012;109:13088–93. https://doi.org/10.1073/pnas.1200791109.
[56] Muhammad MH, Idris AL, Fan X, Guo Y, Yu Y, Jin X, Qiu J, Guan X, Huang T. Beyond risk: bacterial biofilms and their regulating approaches. Front Microbiol 2020;11. https://doi.org/10.3389/fmicb.2020.00928.
[57] Bearon RN, Durham WM. A model of strongly biased chemotaxis reveals the trade-offs of different bacterial migration strategies. Math Med Biol A J IMA 2020;37:83–116. https://doi.org/10.1093/imammb/dqz007.
[58] Alejandro Bonilla F, Kleinfelter N, Cushman JH. Microfluidic aspects of adhesive microbial dynamics: a numerical exploration of flow-cell geometry, brownian dynamics, and sticky boundaries. Adv Water Resour 2007;30:1680–95. https://doi.org/10.1016/j.advwatres.2006.05.028.
[59] Lambert G, Bergman A, Zhang Q, Bortz D, Austin R. Physics of biofilms: the initial stages of biofilm formation and dynamics. New J Phys 2014;16:45005. https://doi.org/10.1088/1367-2630/16/4/045005.
[60] Whiley H, Taylor M. *Legionella* detection by culture and QPCR: comparing apples and oranges. Crit Rev Microbiol 2016;42:65–74. https://doi.org/10.3109/1040841X.2014.885930.
[61] Sylvestre É, Rhoads WJ, Julian TR, Hammes F. Quantification of *Legionella pneumophila* in building potable water systems: a meta-analysis comparing qPCR and culture-based detection methods (pre-print). medRxiv 2024. https://doi.org/10.1101/2024.05.02.24306716.
[62] Pazos-Rojas LA, Cuellar-Sánchez A, Romero-Cerón AL, Rivera-Urbalejo A, Van Dillewijn P, Luna-Vital DA, Muñoz-Rojas J, Morales-García YE, Bustillos-Cristales MDR. The viable but non-culturable (VBNC) state, a poorly explored aspect of beneficial bacteria. Microorganisms 2023;12. https://doi.org/10.3390/microorganisms12010039.
[63] Schrammel B, Cervero-Aragó S, Dietersdorfer E, Walochnik J, Lück C, Sommer R, Kirschner A. Differential development of *Legionella* sub-populations during short- and long-term starvation. Water Res 2018;141:417–27. https://doi.org/10.1016/j.watres.2018.04.027.
[64] Nisar MA, Ross KE, Brown MH, Bentham R, Best G, Eyre NS, Leterme SC, Whiley H. Increased flushing frequency of a model plumbing system initially promoted the formation of viable but non culturable cells but ultimately reduced the concentration of culturable and total *Legionella* DNA. Heliyon 2024;10:e32334. https://doi.org/10.1016/j.heliyon.2024.e32334.
[65] Erdei-Tombor P, Kiskó G, Taczman-Brückner A. Biofilm Formation in water distribution systems. Processes 2024;12:280. https://doi.org/10.3390/pr12020280.
[66] Walker JT, Mackerness C, Rogers J, Keevil CW. Heterogeneous mosaic biofilm - a haven for waterborne pathogens. Microbial Biofilms 1995:196–204.